

## Microscopic Insight into Surface Wetting: Relations between Interfacial Water Structure and the Underlying Lattice Constant

Chongqin Zhu,<sup>1</sup> Hui Li,<sup>1,2</sup> Yongfeng Huang,<sup>1</sup> Xiao Cheng Zeng,<sup>2</sup> and Sheng Meng<sup>1,\*</sup>

<sup>1</sup>*Beijing National Laboratory for Condensed Matter Physics and Institute of Physics, Chinese Academy of Sciences, Beijing 100190, China*

<sup>2</sup>*Department of Chemistry and Nebraska Center for Materials and Nanoscience, University of Nebraska, Lincoln, Nebraska 68588, USA*

(Received 23 October 2012; revised manuscript received 9 January 2013; published 19 March 2013)

We report simulation evidence that the structure of the first water layer next to the surface can strongly affect the contact angle of water droplets. Molecular dynamics simulations show that a small uniform strain ( $\pm 3\%$ ) applied to the lattice constant of a multilayer hydrophilic surface can introduce a marked change in the wetting tendency. In particular, when the lattice constant of a hydrophilic surface matches the projected oxygen-oxygen distance of bulk water to the surface, a contact-angle minimum is resulted. In stark contrast, such a lattice strain has little effect on the wetting properties of hydrophobic surfaces. The structure of the first water layer next to the hydrophilic surface gradually loses characteristics of liquid water when moving away from the contact-angle minimum. Our results demonstrate a close correlation among the length of lattice constant, contact angle of the water droplet, and the structure and dynamics of vicinal water.

DOI: [10.1103/PhysRevLett.110.126101](https://doi.org/10.1103/PhysRevLett.110.126101)

PACS numbers: 68.08.Bc, 61.20.Ja

The wetting property of water has been a topic of wide interest due to its central role in numerous processes in physical, biological, chemical, and technological systems [1–12]. Since almost all wetting processes occur on the surfaces of solids, understanding the relevance between the wetting properties and the structure of interface is a key to study surface wetting. Over the past half century, the physics of wettability as well as general behaviors of water adsorption on surfaces have been intensively investigated [13,14]. As an example, both molecular dynamics (MD) simulations [15,16] and experiments [17,18] have shown evidence of “water monolayer on surface does not wet water,” proving the necessity to understand surface wetting from the perspective of interfacial structure and adsorbate-surface interaction.

However, influence of the *realistic* structure of the first water layer on wettability of a solid surface remains elusive. It has been long debated whether the lattice match of crystal surface to the structure of normal ice  $I_h$  has a positive effect on water wetting and nucleation. In 1947, Vonnegut proposed to use small particles of silver iodide to promote water nucleation in clouds in forming precursors for artificial rainfall [19]. The idea is based on the fact that the lattice parameters of ice  $I_h$  and  $\beta$ -AgI nearly match each other with only 1.6% difference, as well as the assumption that an excellent substrate-ice lattice match promotes wetting. Later, Langmuir tested whether AgI could facilitate monsoon clouds in New Mexico drop rain. However, subsequent experimental studies of ice formation on the hexagonal BaF<sub>2</sub>(111) surface [whose lattice constant (4.38 Å) is within 3% difference to the basal plane of hexagonal ice  $I_h$ ] demonstrated that both the ice

nucleation rate and the onset temperature did not increase (or could even decrease), compared to materials without lattice match [20,21]. According to these early studies, the precise causal relation between surface lattice and water wetting remains ambiguous. Therefore, the notion that lattice match at interface plays an essential role in ice nucleation is largely laid aside.

In this study, we attempt to use atomistic MD simulations to explore the effect of lattice parameters on the wetting property of surface (e.g., degrees of hydrophilicity) by measuring the contact angle (CA) of water droplets on the surface (see Fig. S1 in the Supplemental Material [22]). We find that when continuously expanding the lattice constant of surface from 2.72 Å to 2.90 Å, the CA of a water droplet on a hydrophobic surface increases monotonically with the lattice constant of substrate. In contrast, the CA on the hydrophilic surface first decreases and then increases, yielding a contact angle minimum at 2.80 Å. This interesting behavior is attributed to the fact that atomistic surface structure can notably affect the structure of the first water layer at the water-substrate interface, which in turn dictates the CA of the water droplets. Consequently, hydrophilicity is enhanced when the surface lattice constant matches the ice  $I_h$  structure with an in-plane periodicity of 2.80 Å. In this case, the two-dimensional hydrogen bonding network induced by the perpendicular surface potential is seriously distorted by atomistic interactions between the substrate lattice and vicinal water, yielding a bulklike interface instead of surface-bound dense water layers.

A series of MD simulations of water droplets on model fcc (111) crystal surface have been carried out to study the

effect of surface lattice on contact angles. The surface lattice constant [denoted  $a$ , see Fig. 1(a)] ranges from 2.72 Å to 2.90 Å. Periodic boundary conditions are applied in all three spatial directions. A surface slab with horizontal dimensions of 200 Å × 200 Å, consisting of nine atomic sheets is employed. The thickness of the slab exceeds 20 Å, larger than the employed cutoff radius (10 Å) for the dispersion interaction. Initially a cuboid box of 2000 water molecules with the size of 48.6 Å × 48.6 Å × 26.1 Å is placed at a distance of 2.5 Å above the substrate so that the interaction between the water droplet and its periodic images is negligible.

The flexible simple point charge [23] model is used for water, whereas water-surface interaction is modeled by a 12-6 Lennard-Jones potential with parameters  $\sigma_{SW} = 3.190$  Å,  $\epsilon_{SW} = 0.4$  kcal/mol representing hydrophobic surfaces and  $\sigma_{SW} = 3.190$  Å,  $\epsilon_{SW} = 0.711$  kcal/mol for hydrophilic surfaces. The electrostatic interaction is calculated by using the Ewald summation method. A leapfrog Verlet integration algorithm with a time step of 0.1 fs is chosen. All systems are pre-equilibrated for the first 20 ps at 300 K in a constant volume and constant temperature ( $NVT$ ) ensemble, while the production trajectories are obtained from succeeding 2 ns simulations in a constant volume and constant total energy ( $NVE$ ) ensemble without thermostat controlling [24,25]. All simulations were performed with the GROMACS 4.4.5 package [26].

The CA of a water droplet (denoted  $\theta_c$ ) on either a hydrophobic or hydrophilic surface as a function of the surface lattice constant  $a$  is shown in Fig. 1(b). For  $a$  ranging from 2.72 Å to 2.90 Å, the CA on hydrophobic surfaces increases monotonically from 103° to 110°, due

to the decreasing surface energy per area as the lattice expands. The statistical error in contact angle estimates is less than  $\pm 2^\circ$ . We follow a macroscopic relation of surface wetting, namely, Young's equation,

$$\cos\theta_c = (\gamma_{SV} - \gamma_{SL})/\gamma_{LV}, \quad (1)$$

where  $\gamma_{SV}$ ,  $\gamma_{SL}$ ,  $\gamma_{LV}$  are interfacial tensions between solid and vapor, solid and liquid, and liquid and vapor phases, respectively. It is understood that the expansion of the substrate lattice leads to a significant decrease of  $\gamma_{SV}$ , which is mainly contributed by interactions within the solid substrate itself. However, the solid-liquid interaction, the major part in  $\gamma_{SL}$ , is maintained by the dynamic structure of liquid during lattice expansion. According to Young's equation, an increase in  $\theta_c$  is expected given the decreased  $\gamma_{SV}$  and unchanged  $\gamma_{SL}$ .

Surprisingly, the dependence of  $\theta_c$  on the lattice constant of a hydrophilic surface shows a more complicated relation, where a CA minimum is induced at  $a = 2.80$  Å. In the range of  $a = 2.72$  Å to 2.80 Å,  $\theta_c$  slightly decreases from 60° to 51°. Then,  $\theta_c$  bounces back to 66° at  $a = 2.83$  Å, and increases with further expanding lattice constant from 2.86 Å to 2.90 Å. It is noted that despite the minimum around  $a = 2.80$  Å, the overall trend in the  $\theta_c$  versus  $a$  curve is similar to that for hydrophobic surfaces, that is,  $\theta_c$  increases with  $a$  over the whole range  $a = 2.72$  Å to 2.90 Å—Young's equation still holds by in large. However, the precise value of the contact angles for  $a \leq 2.77$  Å,  $2.77$  Å  $\leq a \leq 2.83$  Å, and  $a \geq 2.83$  Å, deviates significantly from the monotonic behavior, strongly implying that the *macroscopic* picture based on Young's equation is inadequate and a *microscopic* description of surface wetting must be invoked. Note that Young's equation is derived based on an ideal model of solid surfaces such that the surface is rigid, flat, perfectly smooth, and chemically uniform. These assumptions do not hold when surfaces entail physical features at the microscopic scale. As an example, recent experiments have shown that water actually forms droplets on a continuous water thin film supported by self assembled monolayers [18]. This fact cannot be explained by Young's equation, but is supported by theoretical simulations [15], further confirming that Young's equation is inadequate in describing wetting phenomena at microscopic scale.

The simulation result that  $\theta_c$  changes more than 15° within such a small range of surface lattice constant (2.77–2.83 Å) demonstrates that the surface lattice can impose drastic influence on the wetting properties of a hydrophilic surface. Importantly, this main conclusion from our simulation is supported by previous experimental measurements of contact angles of water droplets on electroplated metal thin films [27]. In the experiment, contact angles of water droplets on perfect surfaces of Au, Ag, Pd, and Rh (see Table S1 in the Supplemental Material [22])

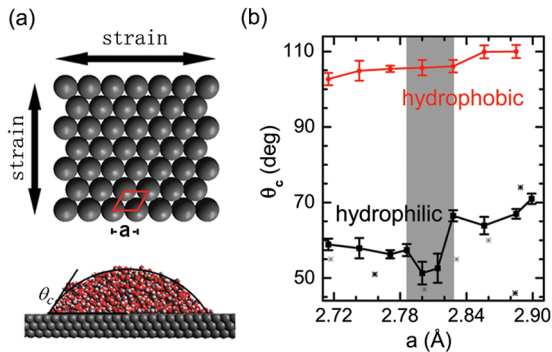


FIG. 1 (color online). (a) Upper panel: The geometry of a model fcc crystal (111) surface. The unit cell with the lattice constant  $a$  is marked. Lower panel: The side view of a water droplet on a model substrate. (b) The contact angle  $\theta_c$  as a function of surface lattice constant for both hydrophilic and hydrophobic surfaces. Black solid squares and red circles represent cases where  $\epsilon_{SW} = 0.711$  kcal/mol and  $\epsilon_{SW} = 0.400$  kcal/mol, corresponding to hydrophilic and hydrophobic surfaces, respectively. Stars denote experimental data of water contact angles on a variety of metal substrates (from Ref. [27], see text).

are measured and compared with those on the corresponding electroplated metal thin films. Because the metal substrates typically impose a strain of 1–3% on the ultrathin electroplated metal films, the contact angles exhibit marked changes (see Table S1 in the Supplemental Material [22]). In addition, we have performed a simple experiment to measure the bending-induced change of a contact angle on Cu foil. We observe that the water CA decreases by about  $4^\circ$  on an inward bent Cu foil but increases by about  $10^\circ$  on outward bent foils (see Fig. S2 in the Supplemental Material [22]). We also note that the minimum in  $\theta_c$  is pronounced since  $\theta_c$  abruptly increases to greater values at the lattice constant, immediately deviating from 2.80 Å (e.g.,  $a = 2.79$  Å and 2.83 Å).

The drastic change in the water contact angle on a hydrophilic surface with the lattice changing from  $a = 2.77$  Å to 2.83 Å, about 6.5 times greater than that for the hydrophobic surface upon the lattice expansion, is correlated with the physics that the interaction between water molecules and the hydrophilic surface is much stronger than that for hydrophobic surface. The water layer next to the hydrophobic surface forms a disordered structure which appears to have negligible influence on the wettability of the surface ( $\theta_c$  changes  $\leq 2^\circ$ ). However, on a hydrophilic surface, our simulation suggests that the structure of the first water layer in contact with the surface can strongly affect its wetting properties.

To find out why hydrophobic and hydrophilic surfaces behave so differently with respect to the expansion of surface lattice and what happens to the first water layer on hydrophilic surface upon the lattice expansion, we have calculated the density of oxygen (black line) and hydrogen atoms (red line) along the surface normal direction, shown in Fig. 2. The first peak centered at the height of 3.0 Å for both O and H profiles exhibits nonmonotonous dependence on the lattice constant  $a$ , where the peak becomes lower and more broadened when  $a$  approaches 2.80 Å and then becomes sharper again. Changes in O and H density profiles are much more pronounced on hydrophilic surfaces than on hydrophobic ones (see Fig. S3 in the Supplemental Material [22]). The sharper primary (or first) peak indicates that a more ordered first water layer is formed, which could lead to surface dewetting due to the distinct structural difference between interfacial water and regular bulk liquid. The same feature also shows up in an oxygen-oxygen radial distribution function (see Fig. S4 in the Supplemental Material [22]). This effect is further demonstrated by the observation that the density of H between the first and second O peaks increases, which implies the number of OH bonds pointing to bulk water increases with increasing  $\theta_c$  when  $a$  deviates from 2.80 Å (see Fig. 2). Similar hydrophobic properties of an ordered water monolayer have been reported with an ionic model substrate [15]. It has been recently established that on ionic substrates there is a critical length for the surface dipoles

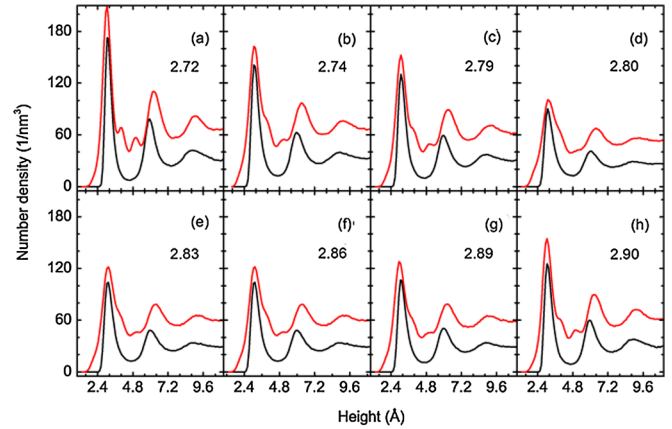


FIG. 2 (color online). Number density of oxygen (black lines) and hydrogen atoms (red lines) in water droplets near the hydrophilic surface. Panels (a) to (h) correspond to  $a = 2.72$  Å, 2.74 Å, 2.79 Å, 2.80 Å, 2.83 Å, 2.86 Å, 2.89 Å, and 2.90 Å, respectively.

below which the wetting properties are not affected by the presence of surface dipole moments [28].

The unusual structure of interface water on hydrophilic surface is further confirmed by the distribution of orientations of water OH groups in the first water layer. Interface water in contact with the substrate has three types of OH groups [29]: OH bonds tangent to surface (denoted T type), OH pointing to the bulk water (denoted B), and dangling OH bonds pointing to the substrate (denoted D). As demonstrated in Fig. 3 and Fig. S5 in the Supplemental Material [22], there are two major peaks at  $25^\circ$  and  $95^\circ$  in the distribution of angle  $\phi$  between the OH bond and the surface normal axis  $z$  for the first water layer, corresponding to OH groups adopting B and T configuration, respectively. The peaks for both B and T types of OH follow the trend of hydrophilicity of the surface, which first become

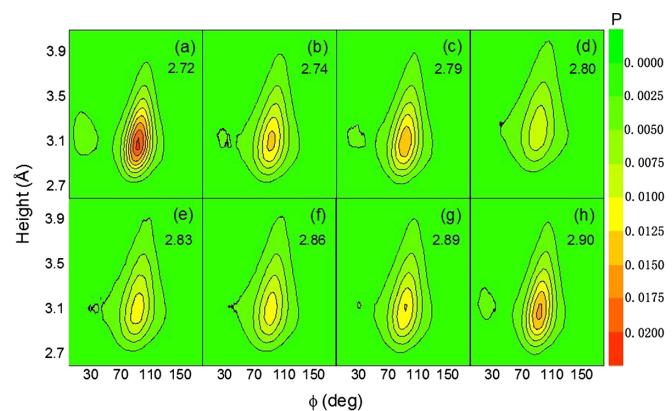


FIG. 3 (color online). Contour distribution of OH orientation for interfacial water molecules as a function of height  $h$  above the substrate and angle  $\phi$ , the angle between the OH group and the surface normal. Panels (a) to (h) correspond to  $a = 2.72$  Å, 2.74 Å, 2.79 Å, 2.80 Å, 2.83 Å, 2.86 Å, 2.89 Å, and 2.90 Å, respectively.

lowered (stronger hydrophilicity) in the range of  $a = 2.72$ – $2.80$  Å [Figs. 3(a)–3(d)], and then become more intense (weaker hydrophilicity) in the range of  $a = 2.83$ – $2.90$  Å [Figs. 3(e)–3(h)]. Consistent with density distribution, more intense peaks indicate that more ordered structure is formed. From Fig. 3, the first water layer at lattice constant  $a = 2.80$  Å exhibits the most disordered structure among all MD simulations. The dynamical instability of such disordered interfacial structure can be also reflected by the reorientation rate of interfacial water molecules, which can be measured by the second order Legendre polynomial time-correlation function (see Fig. S6 in the Supplemental Material [22]). As expected, the highest reorientation rate for interfacial water corresponds to  $a = 2.80$  Å.

An arising question is why is the lattice constant of  $2.80$  Å so special for the structure of interfacial water? It is well known that each water molecule tends to form a transient tetrahedral configuration with four neighbor water molecules in bulk water [30]. Because of the confinement of the substrate, the tetrahedral configuration prefers to adopt the orientation with a  $C_3$  axis perpendicular to the surface. In the present simulation, the average distance between two adjacent oxygen atoms in bulk water is found to be  $2.97$  Å. Considering the tetrahedral configuration, its lateral projection on the solid surface is precisely  $2.80$  Å, corresponding to the lattice constant of the most hydrophilic surface. On hydrophilic substrates, interfacial water molecules tend to adopt a more ordered network structure than bulk water [31,32]. However, this kind of ordered structure can be disrupted by strong atomistic interactions between the substrate lattice and vicinal water molecules. When the surface lattice parameter matches the length scale of projected oxygen-oxygen distance in bulk water, this network structure is maximally distorted due to the combined influence of the potential of surface atoms and bulk water, leading to enhanced disorder in the interfacial water layer. As a result, interfacial water is more bulklike and the hydrophilicity is enhanced. In contrast, interactions between water and atoms of a hydrophobic surface are relatively weak, and the structure of interfacial water is little disturbed, thereby there is little influence of the surface lattice on the water CA.

There are two ways to reduce the ordering of interfacial water: one is through disruption of the network between the first and second water layers, and the other is through the disruption of the network within the first water layer. To determine which one is more important, intra- and inter-layer hydrogen bond (HB) networks of the first water layer are analyzed by counting the HB number versus surface lattice constant, as shown in Fig. 4. In general, the number of HBs formed between the first and second water layers increases with the lattice constant, due to the decreasing interfacial interaction. On the contrary, the number of HBs within the first water layer exhibits a similar trend as the

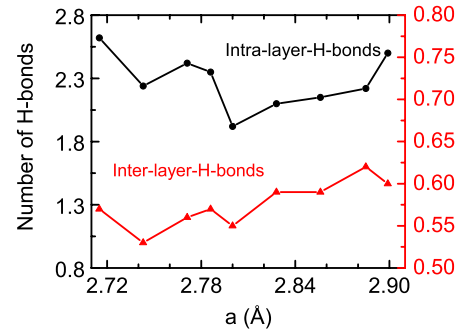


FIG. 4 (color online). Average number of hydrogen bonds formed by a water molecule in the first water layer with other water molecules in the same monolayer (black circles), and with water molecules above the first water layer (red triangles).

changes in hydrophilicity. At  $a = 2.72$  Å, each water molecule is connected to almost three adjacent water molecules via a HB within the same water layer, indicating a perfect tetrahedral configuration is formed with a  $C_3$  axis along the surface normal. However, the number of intralayer HBs per water molecule goes down to less than two at  $a = 2.80$  Å, implying the tetrahedral configuration is significantly disrupted. As the lattice constant is larger than  $2.80$  Å, the number of intralayer HBs increases again. Therefore the lattice-constant match has little effect on interlayer network of water, but it seriously affects the ordering of HB network within the first water layer. This is in stark contrast with droplets on a model ionic substrate, where the number of interlayer (intralayer) HBs keeps increasing (decreasing) with increasing hydrophilicity [15].

The enhancement of in-plane disorder can be seen via comparing the snapshots of the first water layers at

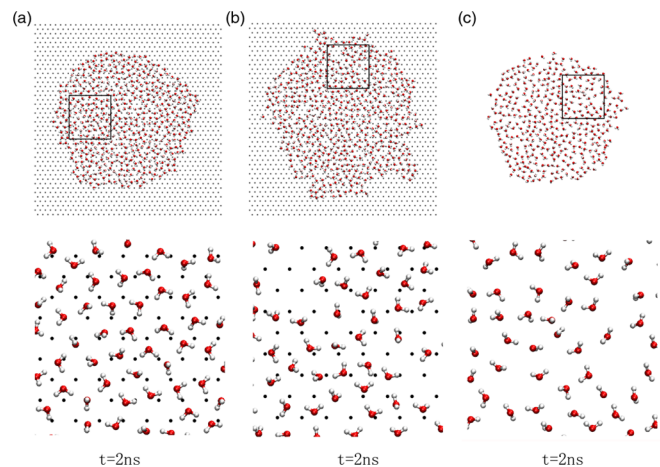


FIG. 5 (color online). Snapshots of the first water layer on the hydrophilic surface at the end of 2 ns on the surface with (a)  $a = 2.72$  Å and (b)  $a = 2.80$  Å. (c) Snapshot of the second water layer on the surface with  $a = 2.72$  Å, which represents the structure of bulk liquid water. The red, white and gray spheres denote oxygen, hydrogen, and surface atoms, respectively.

$a = 2.72 \text{ \AA}$  and  $a = 2.80 \text{ \AA}$  in Fig. 5(a) and 5(b), respectively, as well as the snapshot of the second water layer at  $a = 2.72 \text{ \AA}$  in Fig. 5(c). It is found that water molecules in Fig. 5(a) exhibit higher density than in Fig. 5(b). In addition, no dangling OH bond is observed in Fig. 5(a), whereas water molecules are arranged in perfect rhombic and hexagonal rings, in agreement with recent studies [33]. However, a large amount of defects with dangling OH bonds are observed in Fig. 5(b), similar to the structure of the second layer in Fig. 5(c). Since the water structure in the second layer next to surface is closer to the structure of bulk liquid, the first water layer at  $a = 2.80 \text{ \AA}$  behaves similarly to bulk water. Our second main conclusion that the structure of the first water layer can strongly affect the contact angle of water droplets is consistent with previous simulations that water droplets can exist on a strongly adsorbed water monolayer [15,16]. This conclusion is also supported by previous experiments [17,18] and other simulations [28,29].

In closing, the unexpected nonmonotonic relationship between the water contact angle and surface lattice constant sheds new light on the microscopic picture of surface wetting through understanding the structure of the first water layer as a function of the lattice constant. We note that the length scale from 2.7 to 2.9  $\text{\AA}$  is close to the lattice constant of popular metal surfaces such as Ag and Pt. Thus, we expect that control of surface wetting properties can be achieved experimentally by applying a small strain to metal thin films.

We acknowledge partial financial support from the water-projects cluster and hundred-talent program of CAS, and NSFC (Grants No. 11074287 and No. 11222431) and MOST (2012CB921403). X.C.Z. is supported by Grants from US NSF (No. CBET-1066947), ARL (No. W911NF1020099), the Nebraska Research Initiative, and the USTC ICQD and USTC Qianren-B summer research grant.

\*smeng@iphy.ac.cn

- [1] T. Koishi *et al.*, *Phys. Rev. Lett.* **93**, 185701 (2004).
- [2] S. Meng, Z. Y. Zhang, and E. Kaxiras, *Phys. Rev. Lett.* **97**, 036107 (2006).
- [3] N. Giovambattista, P.G. Debenedetti, and P.J. Rossky, *J. Phys. Chem. B* **111**, 9581 (2007).
- [4] T. Koishi, K. Yasuoka, S. Fujikawa, T. Ebisuzaki, and X. C. Zeng, *Proc. Natl. Acad. Sci. U.S.A.* **106**, 8435 (2009).
- [5] K. Koga, J.O. Indekeu, and B. Widom, *Phys. Rev. Lett.* **104**, 036101 (2010).
- [6] T. Koishi, K. Yasuoka, S. Fujikawa, and X. C. Zeng, *ACS Nano* **5**, 6834 (2011).
- [7] H. Li and X. C. Zeng, *ACS Nano* **6**, 2401 (2012).
- [8] R. Blossey, *Nat. Mater.* **2**, 301 (2003).
- [9] R. Wang, K. Hashimoto, A. Fujishima, M. Chikuni, E. Kojima, A. Kitamura, M. Shimohigoshi, and T. Watanabe, *Nature (London)* **388**, 431 (1997).
- [10] J. Rafiee, X. Mi, H. Gullapalli, A. V. Thomas, F. Yavari, Y. F. Shi, P. M. Ajayan, and N. A. Koratkar, *Nat. Mater.* **11**, 217 (2012).
- [11] C. Duprat, S. Protière, A. Y. Beebe, and H. A. Stone, *Nature (London)* **482**, 10779 (2012).
- [12] R. H. Zhou, X. H. Huang, C. J. Margulis, and B. J. Berne, *Science* **305**, 1605 (2004).
- [13] P. A. Thiel and T. E. Madey, *Surf. Sci. Rep.* **7**, 211 (1987).
- [14] P. J. Feibelman, *Science* **99**, 295 (2002).
- [15] C. L. Wang, H. J. Lu, Z. G. Wang, P. Xiu, B. Zhou, G. H. Zuo, R. Z. Wan, J. Z. Hu, and H. P. Fang, *Phys. Rev. Lett.* **103**, 137801 (2009).
- [16] C. L. Wang, B. Zhou, P. Xiu, and H. P. Fang, *J. Phys. Chem. C* **115**, 3018 (2011).
- [17] G. A. Kimmel, N. G. Petrik, Z. Dohnálek, and B. D. Kay, *Phys. Rev. Lett.* **95**, 166102 (2005).
- [18] M. James, T. A. Darwish, S. Ciampi, S. O. Sylvester, Z. M. Zhang, A. Ng, J. J. Gooding, and T. L. Hanley, *Soft Matter* **7**, 5309 (2011).
- [19] B. Vonnegut, *J. Appl. Phys.* **18**, 593 (1947).
- [20] H. E. Swanson and E. Tatge, *Natl. Bur. Stand. (U.S.)*, *Circ.* **70**, 539 (1953).
- [21] P. Conrad, G. E. Ewing, R. L. Karlinsey, and V. Sadtschenko, *J. Chem. Phys.* **122**, 064709 (2005).
- [22] See Supplemental Material at <http://link.aps.org/supplemental/10.1103/PhysRevLett.110.126101> for experimental data and additional theoretical information.
- [23] O. Teleman, B. Jönsson, and S. Engström, *Mol. Phys.* **60**, 193 (1987).
- [24] T. Werder, J. H. Walther, R. L. Jaffe, T. Halicioglu, F. Noca, and P. Koumoutsakos, *Nano Lett.* **1**, 697 (2001).
- [25] T. Werder, J. H. Walther, R. L. Jaffe, T. Halicioglu, and P. Koumoutsakos, *J. Phys. Chem. B* **107**, 1345 (2003).
- [26] E. Lindahl, B. Hess, and D. van der Spoel, *J. Mol. Model.* **7**, 306 (2001).
- [27] R. A. Erb, *J. Phys. Chem.* **69**, 1306 (1965).
- [28] C. L. Wang, B. Zhou, Y. S. Tu, M. Y. Duan, P. Xiu, J. Y. Li, and H. P. Fang, *Sci. Rep.* **2**, 358 (2012).
- [29] G. Stirnemann, P. J. Rossky, J. T. Hynes, and D. Laage, *Faraday Discuss.* **146**, 263 (2010).
- [30] T. Bartels-Rausch *et al.*, *Rev. Mod. Phys.* **84**, 885 (2012).
- [31] M. C. Gordillo, and J. Marti, *J. Chem. Phys.* **117**, 3425 (2002).
- [32] J. Janecek and R. R. Netz, *Langmuir* **23**, 8417 (2007).
- [33] S. Han, M. Y. Choi, P. Kumar, and H. E. Stanley, *Nat. Phys.* **6**, 685 (2010).